Beam-plasma system as reduced model for ITER relevant energetic particle transport

N. Carlevaro[1,2], G. Montani[1,3], F. Zonca[1,4], P. Lauber[5], T. Hayward-Schneider[5]

[1] *ENEA, FSN Dep., C. R. Frascati, Via E. Fermi 45, 00044 Frascati (Roma), Italy*

[2] *Consorzio RFX, Corso Stati Uniti 4, 35127 Padova, Italy*

[3] *Physics Department, "Sapienza" University of Rome, P.le Aldo Moro 5, 00185 Roma, Italy*

[4] *IFTS and Department of Physics, Zhejiang University, Hangzhou 310027, China*

[5] *Max-Planck-Institut fuer Plasmaphysik, Boltzmannstrasse 2, D-85748 Garching, Germany*

Abstract We provide a mapping procedure to describe the radial profile evolution of energetic particles (EPs) (interacting with Alfvén Eigenmodes (AEs)), by means of an equivalent beam-plasma system (BPS). This technique is applied to reproduce an ITER relevant case, outlining good agreements and relevant deviations from the pure diffusive quasi-linear (QL) evolution.

Beam-plasma interaction We adopt the Hamiltonian formulation and integration methods of the BPS addressed in [1, 2] (and refs. therein). The background plasma is assumed as a 1D cold linear dielectric medium (periodic slab of length L) supporting m longitudinal Langmuir modes $\varphi_j(k_j,t)$, with mode number k_j, while the beam is taken tenuous having density n_B much smaller than the plasma one n_p ($\eta \equiv n_B/n_p \ll 1$). The dynamical equations write as follows:

$$\bar{x}_i' = u_i\,, \qquad u_i' = \sum_{j=1}^{m} \left(i\,\ell_j\,\bar{\phi}_j\, e^{i\ell_j \bar{x}_i} + c.c. \right), \qquad \bar{\phi}_j' = -i\bar{\phi}_j + \frac{i\eta}{2\ell_j^2 N} \sum_{i=1}^{N} e^{-i\ell_j \bar{x}_i} - \bar{\gamma}_{dj}\bar{\phi}_j\,. \tag{1}$$

Beam particle positions (velocities) are labeled by x_i (v_i) (N being the total particle number) and scaled as $\bar{x}_i = x_i(2\pi/L)$ ($u_i = \bar{x}_i' = v_i(2\pi/L)/\omega_p$). The plasma frequency is ω_p and $\tau = t\omega_p$ (the prime indicates τ-derivative). Moreover $\ell_j = k_j(2\pi/L)^{-1}$, $\phi_j = (2\pi/L)^2 e\varphi_j/m_e\omega_p^2$ and $\bar{\phi}_j = \phi_j e^{-i\tau}$, while barred frequencies and growth rates are in ω_p units. In particular, we include in the dynamics an external damping rate $\bar{\gamma}_{dj}$ for each mode. Linearly unstable modes satisfy the resonance conditions $\ell_j u_{rj} = 1$ (u_r denotes a resonant velocity) and we deal with a warm beam initially distributed with a given $F_{B0}(u)$ in the velocity space. Linear drives $\bar{\gamma}_{Dj}$ are defined by means of the dimensionless dispersion relation (here $M = \int du F_{B0}$)

$$2(\bar{\omega}_{0j} + i\bar{\gamma}_{Dj} - 1) - \frac{\eta}{\ell_j M} \int_{-\infty}^{+\infty} du \frac{\partial_u F_{B0}(u)}{u\ell_j - \bar{\omega}_{0j} - i\bar{\gamma}_{Dj}} = 0\,, \tag{2}$$

where the dielectric is expanded near $\bar{\omega} \simeq 1$ (according to the motion equations (1)) and we use $\bar{\omega} = \bar{\omega}_0 + i\bar{\gamma}_D$. The effective mode growth rates are, thus, $\bar{\gamma}_j = \bar{\gamma}_{Dj} - \bar{\gamma}_{dj}$. We also note that the non-linear spread Δ_{NLj} of beam particle due to the resonant interaction with a single given mode results proportional to the growth rate [3], *i.e.,* $\Delta_{NLj} \propto \bar{\gamma}_j/\ell_j$.

Mapping procedure We now describe the technique to map the reduced radial profile of the burning plasma scenario to the velocity space of the BPS. This corresponds to a one-to-one link, once the EP/AE system is dimensionally reduced by using suitable averaged distribution functions. The map should be defined for a single reference resonance (resulting in a linear relation then extended to the multi-mode case) by preserving non-linear particle redistribution (for an application to the nonlinear dynamics of EP driven geodesic acoustic modes, see [4]).

For a chosen reference resonance (dropping the j index), the map is derived using resonance conditions $\bar{\omega}^{AE}(s) - \bar{\omega}^{AE}(s_r) \propto \ell(u - u_r)$, where ω^{AE} is the AE frequency and the subscript r indicates the resonance value of a quantity. Here, the normalized Tokamak radius reads $s = r/a$ (a is the minor radius), while, barred frequencies (growth rates and damping) are in ω_{A0} unities, where $\omega_{A0} = v_{A0}/R_0$ (v_{A0} is the Alfvén speed at the magnetic axis and R_0 the major radius). Furthermore, n^{AE} will denote the toroidal mode number. We address a local map trough the linear expansion $\bar{\omega}^{AE}(s) = \bar{\omega}^{AE}(s_r) + (s - s_r)\partial_s \bar{\omega}^{AE}$: imposing boundary conditions $s = 0 \mapsto u = u_{max}$ and $s = 1 \mapsto u = 0$, the relation between velocity and radial profile finally writes

$$u = (1 - s)/\ell_1 \,, \tag{3}$$

where ℓ_1 is an arbitrary parameter related to the periodicity length L of the BPS 1D slab. The BPS can be properly simulated once the density parameter η is fixed in Eqs.(1) and it is important to stress how the EP/AE system has an higher dimensionality (3D). In this respect, the EP response is intrinsically different: in the BPS no modulation of power exchange is present, dealing with only one class of resonant particles. Thus, the transport results more efficient for equal drive. In order to qualitatively compare the non-linear redistribution of the two systems, we impose that linear drives normalized to the mode frequencies are proportional, *i.e.,* $\bar{\gamma}_D/\bar{\omega}_0 = \alpha\, \bar{\gamma}_L^{AE}/\bar{\omega}^{AE}$, with $\alpha \leqslant 1$ to reduce the drive in the BPS simulations. The η parameter is now given integrating Eq.(2) with $F_{B0}(u) \to F_{H0}(s)$ (assigned initial EP radial profile). This closes the single mode mapping and the whole spectrum is addressed using resonance conditions: $\ell_j = \ell_1/(1 - s_{rj})$. Finally, to preserve asymptotic mode decay, we set $\bar{\gamma}_{dj}/\bar{\omega}_{0j} = \bar{\gamma}_{dj}^{AE}/\bar{\omega}_j^{AE}$.

We conclude by writing the mapped QL evolutive equations [5] for the EP profile $f_H(\tau, s)$:

$$f_H = F_{H0} - \pi \bar{\mathcal{N}} R \partial_s [(1 - s)^{-5} \bar{\mathscr{I}}] \,, \tag{4a}$$

$$\partial_\tau \bar{\mathscr{I}} = -\eta R^{-1} (1 - s)^2 \bar{\mathscr{I}}\, \partial_s F_{H0} + \pi \eta (1 - s)^2 \bar{\mathcal{N}}\, \bar{\mathscr{I}}\, \partial_s^2 [(1 - s)^{-5} \bar{\mathscr{I}}] \,, \tag{4b}$$

where $R = \int ds F_{H0}$, while the spectrum is $\bar{\mathscr{I}}(\tau, s) = \ell_1^5 |\bar{\phi}|^2/\eta$ ($\bar{\phi}(\tau, s)$ is the continuous spectrum derived from the discrete one, specified by means of resonance conditions). We have defined also the spectral density $\bar{\mathcal{N}} = m/\Delta\ell$ (with $\Delta\ell = \mathrm{Max}[\ell_j] - \mathrm{Min}[\ell_j]$ denotes the spectral width).

Application to a realistic case We now apply the mapping technique above to the reduced ITER 15MA beseline scenario in [6]. In particular, we run simulations for the BPS Eqs.(1) mapped back to the normalized radial dimension. We deal with an initial EP slowing down $F_{H0}(s)$, with the least damped 27 toroidal AEs (TAEs) (Fig.1, left panel): $n^{AE} \in [12,30]$ (main branch) and $n^{AE} \in [5,12]$ (low branch, almost linearly stable). The reference resonance is set

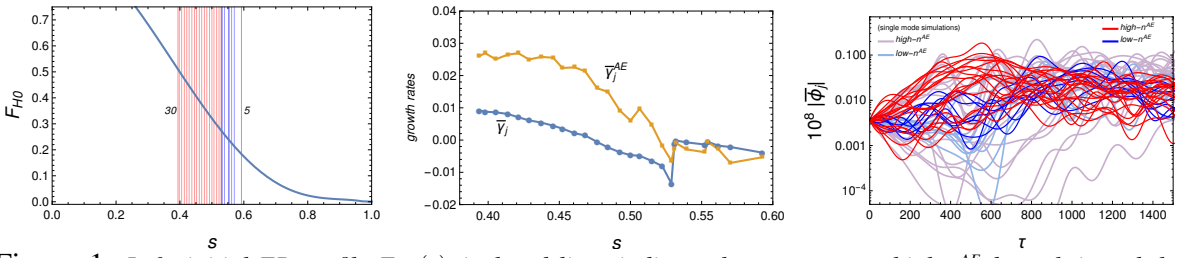

Figure 1: *Left: initial EP profile $F_{H0}(s)$ (colored lines indicate the resonances: high-n^{AE} branch in red, low-branch in blue). Center: growth rates $\bar{\gamma}_j$ and $\bar{\gamma}_j^{AE}$, for $\alpha = 0.4$. Right: Self-consistent evolution of the 27 modes (bright colors) plotted over the correspondent single mode behaviors (opaque colors).*

$n^{AE} = 21$ and we consider $\alpha = 0.4$ to obtain optimized EP profiles with respect to [6]. Thus, we get $\eta \simeq 0.07$ and, by integrating Eq.(2) and setting the damping profile, we obtain the growth rates in Fig.1, center panel, plotted with the corresponding $\bar{\gamma}_j^{AE}$ for the TAEs. The growth rate profile results reliable for the main branch (considering the scaling), while the discrepancy for the low branch is due to the $\bar{\omega}^{AE}$ changes, not accounted in the BPS, *i.e.*, $\bar{\omega}_{0j} \sim 1 \forall j$.

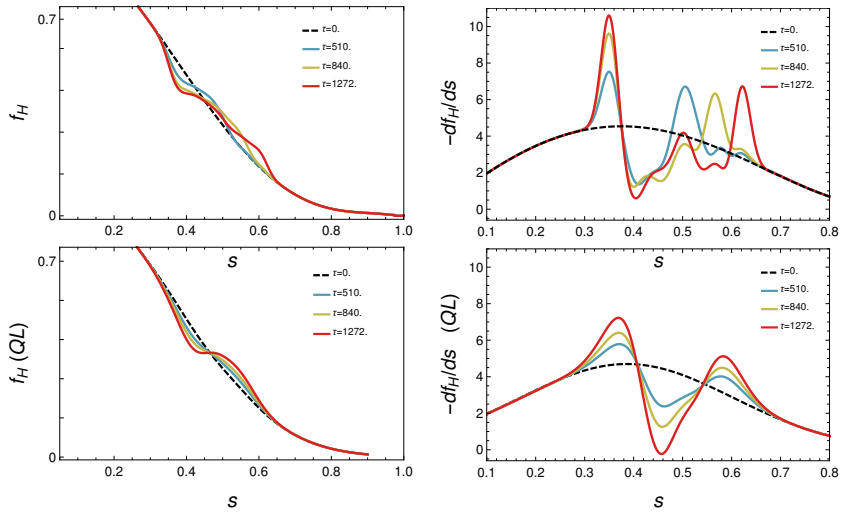

Figure 2: *Upper panels: EP profile (left) and its radial gradient (right) at different times. Lower panels: EP redistribution (left) and its radial gradient (right) as evolved from QL model (4) for the same times.*

In Fig.1, right panel, we compare 27 runs of single mode (opaque colors) to the multi mode simulations (bright colors). As a result, the low-branch (blue) is more efficiently exited in the multi mode dynamics, despite the negative drive. This feature is in perfect agreement with [6] and it is due to an avalanche particle transport in the correspondent resonance radial portion. Such a spectral behavior reflects on the EP profile $f_H(s)$ evolution, plotted in Fig.2, upper left

panel, together with its radial gradient (upper right). Transport toward large s is clearly outlined, in particular, a second peak (resonating with the low branch) is shifting toward $s \simeq 0.65$.

We now compare the QL evolution, by integrating Eqs.(4) using the same initial F_{H0} and a Gaussian profile for $\bar{\mathscr{J}}(0,s)$ to model the discrete mode spectrum. The results are given in Fig.2, lower panels: the avalanche and the related radial transport is absent, outlining, as in Ref.[6], the convective evolutive character not reproducible with a pure diffusive QL model.

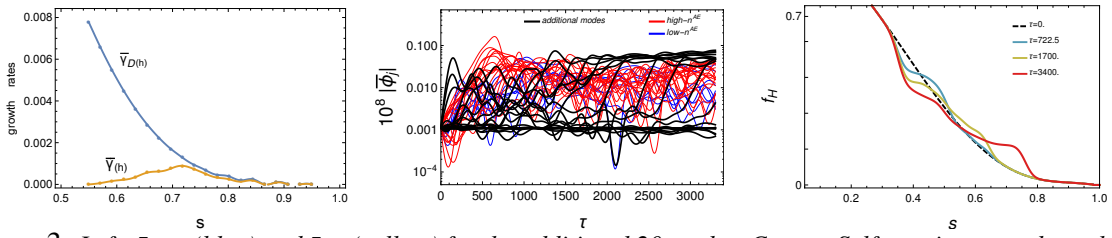

Figure 3: *Left: $\bar{\gamma}_{D(h)}$ (blue) and $\bar{\gamma}_{(h)}$ (yellow) for the additional 20 modes. Center: Self-consistent mode evolution. Right: EP redistribution for the same times of Fig.2.*

In the self-consistent analysis, since we are dealing a chosen fixed spectrum (Fig.2, upper panels), EP transport results bounded due to the absence of further unstable modes. In fact, an outer redistribution around $s \simeq 0.85$ is found in [6], and this discrepancy is due to the poloidal harmonics spectrum filling a wide resonance region. To model this feature, we include 20 additional modes resonating in $0.55 \leqslant s \leqslant 0.95$: each mode has a drive $\bar{\gamma}_{D(h)}$ ($h = 1, ..., 20$) from Eq.(2) and, to reproduce the morphology of the harmonic spectrum, we address damping rates $\bar{\gamma}_{d(h)}$ giving rise to Gaussian distribution for $\bar{\gamma}_{(h)} = \bar{\gamma}_{D(h)} - \bar{\gamma}_{d(h)}$ (Fig.3, left panel). From the simulation results, the spectral transfer clearly emerges (Fig.3, center panel): the additional modes are progressively exited producing an increased avalanche transport toward large radial positions (Fig.3, right panel).

Concluding remarks Nonetheless the agreement of the mapping procedure compared to [6] is on a qualitative level, the merit of this analysis is to underline and confirm the effective mechanism yielding non-pure diffusive transport: the presence of neighboring resonances in the spectrum induces avalanche processes able to trigger EP transport toward the edge.

References

[1] N. Carlevaro, M.V. Falessi, G. Montani, F. Zonca, *J. Plasma Phys.* **81**(5), 495810515 (2015).

[2] N. Carlevaro, A.M. Milovanov, M.V. Falessi, G. Montani, D. Terzani, F. Zonca, *Entropy* **18**(4), 143 (2016).

[3] N. Carlevaro, G. Montani, F. Zonca, in *45th EPS Conference on Plasma Physics 2018*, **42A**, P5.1067.

[4] A. Biancalani, N. Carlevaro, A. Bottino, G. Montani, Z. Qiu, *J. Plasma Phys.* **84**(6), 725840602 (2018).

[5] G. Montani, F. Cianfrani, N. Carlevaro, *Plasma Phys. Contr. Fus.* **61**, 075018 (2019).

[6] M. Schneller, Ph. Lauber, S. Briguglio, *Plasma Phys. Contr. Fus.* **58**, 014019 (2016).

This work has been carried out within the framework of the EUROfusion Consortium [ER Projects: NAT (AWP17-ENR-MFE-MPG-01), MET (CfP-AWP19-ENR-01-ENEA-05)] and has received funding from the Euratom research and training programme 2014-2018 and 2019-2020 under grant agreement No 633053. The views and opinions expressed herein do not necessarily reflect those of the European Commission.